

Response to reviewer # 1

K. Rypdal¹

¹Department of Mathematics and Statistics, UiT The Arctic University of Norway, Norway

Correspondence to: Kristoffer Rypdal
(kristoffer.rypdal@uit.no)

Thanks for a constructive review. My response to the reviewer's comments and how they will be adopted in the revised manuscript can be found below.

1. *Reviewer*: Please define AD.

Response: This will be done. Actually, there are different conventions, and the usage of AD (Anno Domini) should be done by placing it before the year (e.g., AD 1880), not after as I have done. A more neutral convention is to use CE (Common Era), which is placed after the year (e.g., 1880 CE). In the revision I will adopt the latter.

2. *Reviewer*: Please define in detail the meanings of fingerprint and footprint.

Response: I think the meaning I give to these words are clearly explained in the text, but I will include some more discussion. In particular because the word "climate footprint" is used in the literature in the meaning of the contribution of specific human activities to the increase in greenhouse gas concentrations. The meaning I give to the fingerprint concept is essentially the same as presented in Chapter 10 on "Detection and Attribution" in the IPPC AR5, WG1, although my usage is simpler since I don't employ principal component analysis or other noise reducing techniques prior to extracting the fingerprint. The usage of the word footprint is not conventional. Reviewer #2 finds it "a little silly," and suggest to replace it by "forcing function" or "response function." In my response to Reviewer #2, I explain why I don't find any of these terminologies adequate. I will also explain in more detail why I use this terminology in the revised manuscript.

3. *Reviewer*: Page 1311, line 15-17: I don't understand this sentence. Attribution does not necessarily only refer to anthropogenic changes, so also internal modes can cause global temperature changes which are attributable.

Response: I don't see the problem here. What the reviewer writes is essentially the same as what I write, except that the word "anthropogenic" has no place here. Anthropogenic causes are treated on the same footing as natural ones. My point is that statistical inference like multiple, linear regression does not establish a causal link, but

rather establishes a statistical model where the observation is expressed as a linear combination of predictor functions (here called fingerprints). These predictor functions may be components of the forcing, and for those cases the attribution is causal. But predictor functions can also be characteristic signatures (fingerprints) of internal modes, which may be established from theory or observation of another climate variable than the one we are modelling. In the latter case we postulate a link (correlation) between the predictor and the modelled variable (predictand), but this link does not have to be causal in the sense that the predictor causes the response. They can for instance have a common cause. This is also discussed on page 1320, lines 24-27.

4. *Reviewer*: Page 1316: Fig. 6a is referenced before Figs. 3-5.

Response: Yes, I know that this is not formally right. But I just wanted to point out that this also is done in Fig. 6a and c, which deals with a different data set. I cannot move this figure, so the alternative is not to mention Fig. 6 here.

5. *Reviewer*: Page 1320: Empirical mode decomposition should be explained and referenced.

Response: The empirical mode decomposition is just one of many decomposition methods that give very similar results, so I rather rephrase the paragraph than digress on this particular method.

6. *Reviewer*: The LM model diverges for large times. I think it would be good if the reasons for this would be discussed. Is this due to missing nonlinear effects/feedbacks in the model? Or is this the imprint of the non-stationarity of a long-memory climate?

Response: The LM response diverges for large times only if the forcing is permanently changed, i.e. if the time-average over a wide time-window is changed. The model is intended to be a simple one-parameter representation of the temperature response valid only within a certain range of scales. One way to think about it is that it describes a linear system involving a hierarchy of exponential responses. It can be shown that such a system is distinguishable from a system with power-law response up to the

largest exponential response time time. Hence, the power-law kernel should be cut off at certain scale. In Rypdal and Rypdal, J. Climate (2014) we investigated this question, and showed that this cut-off scale should be larger than several centuries in order for the model to predict the Moberg record with acceptable accuracy. I see no reason to repeat that discussion in this paper, but in the revision I have expanded the discussion of the long-term effect of an initial radiative imbalance.

7. *Reviewer*. Figure axes: I would prefer if the figure axis would be labeled with absolute years instead of relative.

Response: I will fix that.

10 *Acknowledgements*. This work was funded by project no. 229754 under the the Norwegian Research Council KLIMAFORSK programme.

Response to reviewer # 2

K. Rypdal¹

¹Department of Mathematics and Statistics, UiT The Arctic University of Norway, Norway

Correspondence to: Kristoffer Rypdal
(kristoffer.rypdal@uit.no)

Reviewer: I agree with reviewer #1's comments, especially the use of the terms fingerprint and footprint. I actually find the transformation of a fingerprint into a footprint a little silly. Perhaps the authors could come up with better words. I prefer using "forcing function", "response function" etc., though I know it is not usually defined to be completely equivalent.

5
Response: I think the meaning I give to these words are clearly explained in the text, but I will include some more discussion in the revision. In particular because the word "climate footprint" is used in the literature in the meaning of the contribution of specific human activities to the increase in greenhouse gas concentrations. The meaning I give to the fingerprint
10 concept is essentially the same as presented in Chapter 10 on "Detection and Attribution" in the IPPC AR5, WG1, although my usage is simpler since I don't employ principal component analysis or other noise reducing techniques prior to extracting the fingerprint. My usage of the word footprint is not conventional. I will explain below why I have used it, but first discuss the reviewer's suggestions and other alternatives.

15 What we are discussing is to find an appropriate word that names the various components of the "explained signal" (or "response variable" or "predictand") in a linear regression. "Forcing function" is very misleading, for two reasons. One is that it will give the impression that the footprints represent the forcing, which it does not. When the fingerprint arises from a forcing the corresponding footprint represents the *the response* to that forcing. But some
20 footprints are not necessarily the response to a forcing, which is the case if it represents an internal mode. "Response function" (or rather "response variable") is better than "forcing function," but I think that "response function" is a misnomer in the statistics literature, because "response" is associated with cause-effect linkage. This is as bad as assuming that correlation implies causation.

25 This paper is not written for statisticians, and I have in mind that the main results should be accessible even for non-scientists. I therefore try to avoid too much of the statistics jargon. Lay-people understand that a fingerprint is a weak signal that contains a lot of information, and is therefore suitable for detection. A footprint is influenced by the weight of the person that makes it, and as an allegory it is used to indicate *an effect, or an imprint*. This

30 is exactly the way I use this word in this paper. I am therefore not willing to drop the usage of these words, but I can add some more discussion of their meaning.

Reviewer: What I would like to see added is a discussion of the physical origin of the time scales involved in the temperature response. Especially, why should we expect these time
35 scales to be the same for the different components? . . . This perhaps is even more so with the AMO and Nino heat exchange with the ocean.

Response: In principle it would be possible to introduce different response times (for SRM) or scaling exponents (for LRM) for different forcings. But this would create more complex
40 models, and if these exponents are treated as regression coefficients, more unknown parameters and increased chance of overfitting. Going to this kind of complexity would make the kind of study I have made here pointless, and full GCM-type modelling would be better. Here there already exist a vast literature.

When it comes to “the AMO and Nino heat exchange with the ocean,” I don’t see the
45 relevance. Here the indices themselves have been used as fingerprints (predictors), and hence there is no response model, and hence no response times, involved.

Reviewer: Regarding the many internal variations (or modes of oscillation, if you want), it should be discussed why AMO and Nino are the ones chosen. Nino I can understand, as
50 it is the biggest reorganization of heat. It seems that the AMO is “convenient” since it is the only one of the five forcing component, which seems to be correlated with the warm forties/cold sixties seen in the global temperature.

Response: I have discussed why I have chosen those two modes, and it is true that the
55 AMO is chosen because it carries an obvious long-time scale signature of the instrumental record. This is a dubious thing only if one interprets attribution as causation. I have been very clear on emphasizing that this analysis does not imply that AMO is the cause of the large scale variability in GMST, only that using this signal obtained by probing the Atlantic

60 SST serves as a good predictor for these features of the GMST. I could have done the same with the PDO, and found that it is not that good a predictor, because the phase-match with the GMST is not so good. That would have been an interesting result too, but then I could go on and include all known modes in the climates system, which wouldn't make much sense.

Acknowledgements. This work was funded by project no. 229754 under the the Norwegian Research Council KLIMAFORSK programme.

Interactive
Comment

Interactive comment on “Attribution in the presence of a long-memory climate response” by K. Rypdal

dr. Rypdal

kristoffer.rypdal@uit.no

Received and published: 25 October 2015

Thanks for an informative and constructive review.

1. Unfortunately, I was not aware of the very comprehensive paper by Canty et al., and it certainly needs to be cited and commented.
2. My formulation “little physical justification” (of delays) was referring to the cited papers by Lean and Rind, and Foster and Rahmstorf, and my concern was mainly the long delay of a decade for the response to anthropogenic forcing. I am not aware of physical justifications of this delay in the mainstream literature. The delays of 1-6 months of response to solar, volcanic and ENSO is not a concern in my paper because I analyse annual time series. The reason for using annual series is that I am concerned

Full Screen / Esc

Printer-friendly Version

Interactive Discussion

Discussion Paper



with effects of long-memory response, and introducing higher resolution and delays of a few months as free parameters will increase the chance of overfitting. In my paper the long delay in the response to anthropogenic forcing is incorporated in the long-memory response.

3. I will cite Canty et al. on this point of the short-time temperature response around volcanic eruptions.

4. It also seems resonable to cite Canty et al. on the need to introduce AMV as a predictor in the regression model.

5. I think I have to choose my wording more carefully. Climate forcing is a problematic concept, since it depends on what one defines as the "system" that is subject to external forcing. As a physicist/applied mathematician who has entered climate science via a non-standard route, I tend to think about ENSO and AMV as internal modes, and not as forcings. But realise that it may be reasonable to think of the Earth surface/mixed layer as the system, and that this system can be forced by modes involving energy exchange between the surface/mixed layer and atmospheric systems (ENSO) and between the surface/mixed layer and the deep ocean (AMV via AMOC). In that case my remarks become rather irrelevant. However, from a mathematics/statistics point of view it may be in place with a reminder that high explained variance associated with a certain predictor variable does not necessaril imply a causal link, and in particular not that the predictor is forcing the reponse variable.

6. It is nice that others reach similar conclusions about the hiatus.

I will certainly discuss Canty et al. also in the concluding section.

Interactive comment on Earth Syst. Dynam. Discuss., 6, 1309, 2015.

Full Screen / Esc

Printer-friendly Version

Interactive Discussion

Discussion Paper



Interactive
Comment

Interactive comment on “Attribution in the presence of a long-memory climate response” by K. Rypdal

dr. Rypdal

kristoffer.rypdal@uit.no

Received and published: 26 October 2015

In my reply I wrote about the decadal delay to anthropogenic forcing: "I am not aware of physical justifications of this delay in the mainstream literature." This is wrong, it was explicitly represented as a result of ocean heat uptake by Canty et al. (2013). I will mention that in the revision.

Interactive comment on Earth Syst. Dynam. Discuss., 6, 1309, 2015.

Full Screen / Esc

Printer-friendly Version

Interactive Discussion

Discussion Paper



Markup-file of revised manuscript

Passages marked in red in the manuscript file below are added in response to the comments from the reviewers.

Attribution in the Presence of a Long-Memory Climate Response

K. Rypdal¹

¹Department of Mathematics and Statistics, UiT The Arctic University of Norway, Tromsø, Norway

Correspondence to: Kristoffer Rypdal
(kristoffer.rypdal@uit.no)

Abstract. Multiple, linear regression is employed to attribute variability in the global surface temperature to various forcing components and prominent internal climatic modes. The purpose of the study is to assess how sensitive attribution is to long-range memory (LRM) in the model for the temperature response. The model response to a given forcing component is its fingerprint, and is different for a zero response-time (ZRT) model and one with LRM response. The fingerprints are used as predictors in the regression scheme to express the response as a linear combination of footprints. For the instrumental period 1880 – 2010 CE the LRM response model explains 89% of the total variance and is also favoured by information-theoretic model-selection criteria. The anthropogenic footprint is relatively insensitive to LRM scaling in the response, and explains almost all global warming after 1970 CE. The solar footprint is weakly enhanced by LRM response, while the volcanic footprint is reduced by a factor of two. The natural climate variability on multidecadal time scales has no systematic trend and is dominated by the footprint of the Atlantic Multidecadal Oscillation. The 2000 – 2010 CE hiatus is explained as a natural variation. A corresponding analysis for the last millennium is performed, using a Northern Hemisphere temperature reconstruction. The Little Ice Age (LIA) is explained as mainly due to volcanic cooling or as a long-memory response to strong radiative disequilibrium during the Medieval Warm Anomaly, and is not attributed to the low solar activity during the Maunder minimum.

1 Introduction

There will always be variability in the Earth’s climate, even in the absence of external forcing like variation in solar irradiance, volcanic eruptions, or human-induced changes. The nature of internal climate variability is analogous to the change of weather, just extrapolated to longer spatial and temporal scales. This “song of Nature” is comprised of a cacophony of frequencies corresponding to the natural modes of the climate system and forms a background spectrum with a pink-noise character. This means that the power spectral density (PSD) of global temperature to a crude approximation has the form $S(f) \sim 1/f$ for frequencies f corresponding to periods from months to millennia. The shape of this spectrum implies that internal variability on low frequencies (long time scales) is

strong, and this constitutes a problem when we want to detect climate signals and trends with external causes. Another complication is that there are also internal modes that stand out of this noise, and the separation of these modes from the noise background is not unique and depends on how the noise is modeled.

Signal detection means to establish the statistical significance of a trend, an oscillation, or a spatiotemporal pattern. This is successfully done if we can establish that it is very unlikely that the pattern, or *fingerprint*, has arisen by chance from the internal background noise. Once fingerprints have been successfully detected, the next issue is to assess their relative weights, or *footprints* in the total climate signal. This process is what we call attribution. A particular footprint can in some cases be perceived as the result of a particular cause, such as a well-identified radiative forcing. In that case the footprint can be thought of as the global temperature response to this particular forcing. But attribution does not have to be causal, which is the case if the footprint is the global temperature manifestation of an internal climate mode. For such a mode, a particular climatic variable or index can serve as a particularly sensitive gauge for this specific mode, and its contribution to the variance of the global temperature signal is the mode's footprint.

A standard method in attribution studies is that of multiple linear regression. The idea is to separate the climate signal into a number of components assumed to represent the climate response to individual forcings in addition to a few prominent internal modes. Each of these components has a certain characteristic fingerprint. In order to determine these fingerprints we need models of some sort. Full-scale AOGCMs can be used, but often also simpler, conceptual models are useful. The rationale for attribution studies is that even the most advanced climate models may estimate wrongly the magnitude of individual responses, even though they have got the fingerprints right. Hence we may write the total climate signal $T(t)$ as a linear combination of the fingerprints. The validity of the linear approximation for global climate variables has been documented in AOGCM-studies by Meehl *et al.* (2004). Consider, for instance, the global temperature $T(t)$ and the fingerprints of various forcings and internal modes. Then we may, for instance, select the following model for the explained global surface temperature (this is also called *the response variable* or *the predictand*);

$$T_{\text{exp}}(t) = f_{\text{sun}} S(t) + f_{\text{volc}} V(t) + f_{\text{anthr}} H(t) + f_{\text{AMO}} A(t) + f_{\text{ENSO}} E(t), \quad (1)$$

where $S(t)$, $V(t)$, $H(t)$ are the fingerprints of solar, volcanic, and human-induced (anthropogenic) forcing, and $A(t)$ and $E(t)$ are the fingerprints of the Atlantic Multidecadal Oscillation (AMO) and the El Niño Southern Oscillation (ENSO), respectively. In regression theory the fingerprints are also called *predictors*. The fitting parameters (or *regressors*) $f_{\text{sun}}, f_{\text{volc}}, \dots$ represent the weight of each fingerprint in the total response, and can be estimated by minimising the least square error with respect to the observed data. These weights take into account that we may not have modeled the magnitude of the individual forcings right, or that we have overlooked, or modelled incorrectly, cli-

mate feedbacks that operate differently for each forcing. A third possible cause of changed weights is incorrect modeling of the temporal response to the forcing. This will give rise to distorted fingerprints. A measure of how successfully the method attributes variability to the various forcing components is to compute how much of the observed variance that is explained by the model.

One common problem with this approach is that if there are many causal factors to consider, and hence many parameters to fit, there is a risk of overfitting. This means that a good fit can be obtained even when the result is unphysical. Another problem is that the fingerprints of forcing in general are distorted and delayed by inertia in the climate response caused by slow heat exchange between the ocean surface layer and the deep ocean, sea ice, and ice sheets. This inertia may, for instance, lead to a small response to the relatively fast solar cycle forcing, while the response to slow trends in solar irradiance may be stronger, but considerably delayed.

Delay effects are generally not accounted for in the regression model Eq. (1) if the model defining the fingerprint does not involve a dynamic response to forcing. Some authors include delays by introducing a fixed time shift which is different for each fingerprint (*Lean and Rind*, 2008, 2009; *Foster and Rahmstorf*, 2011). In these papers delays are introduced for the sole purpose to improve the fit and they increase the number free parameters in the regression model. Under any circumstance, the delay introduced for volcanic, solar, and ENSO fingerprints are a few months, and hence are not detectable in the present analysis, which deals with annual data. However, a decadal delay for the anthropogenic fingerprint found by *Lean and Rind* (2008, 2009) was explicitly represented as a result of ocean heat uptake by *Canty et al.* (2013). In the present paper this delay due to heat exchange with the deep ocean is represented by the long-memory response. The response function to all forcing components are assumed to have the same shape, and involves distortion, not just shifts, of the forcing signals. A conceptual stochastic-dynamic model of such a long-memory dynamic response is described in *Rypdal and Rypdal* (2014), where it is shown that for the global temperature this model provides results that are essentially indistinguishable from those obtained from the Coupled Model Intercomparison Project Phase 5 (CMIP5) ensemble of general circulation models for the industrial period with historical forcing.

In its most simple form the stochastic-dynamic model is a zero-dimensional energy-balance model (EBM) on the form

$$\frac{dT}{dt} = -\frac{1}{\tau}T + F_{\text{det}}(t) + \sigma w(t), \quad (2)$$

where $T(t)$ is a perturbation of the surface temperature from an equilibrium state, $F_{\text{det}}(t)$ is the total deterministic forcing, $\sigma w(t)$ is a white-noise stochastic forcing, and $-(1/\tau)T(t)$ the radiation imbalance at the top of the atmosphere. The solution if $T(0) = 0$ is

$$T(t) = \underbrace{\int_0^t G(t-t')F_{\text{det}}(t') dt'}_{T_{\text{det}}(t)} + \sigma \underbrace{\int_0^t G(t-t') w(t') dt'}_{T_{\text{stoch}}(t)}, \quad (3)$$

where the response function $G(t) = c \exp(-t/\tau)$ represents the impulse response to a delta-function forcing, and hence τ is the characteristic damping time (time constant). It depends on the effective heat capacity C_{eff} of the combined land and ocean surface layer and the climate sensitivity S as $\tau = C_{\text{eff}} S$. The first term $T_{\text{det}}(t)$ on the right hand side is the temperature response to the known (deterministic) forcing. The second term $T_{\text{stoch}}(t)$ is the Ornstein-Uhlenbeck (OU) stochastic process, which in discrete time reduces to the first-order autoregressive (AR(1)) process. This process is stationary and has an autocorrelation function (ACF) on the form $C(t) \sim \exp(-t/\tau)$. The PSD of this process has the shape of a Lorentzian distribution; it is flat ($S(f) \sim f^0$) for $f \ll \tau^{-1}$ and decays as $S(f) \sim f^{-2}$ for $f \gg \tau^{-1}$. If Eq. (3) were a good model for the global surface temperature, the residual $T_{\text{obs}}(t) - T_{\text{det}}(t)$ should correspond to T_{stoch} , and hence be successfully modeled as an OU process. In *Rypdal and Rypdal* (2014), however, it was shown that this residual does not have a Lorentzian PSD, but rather exhibits the power-law form $S(f) \sim f^{-\beta}$, with $\beta \approx 0.75$. This is a persistent process that exhibits long-range memory, and is called a *fractional Gaussian noise* (fGn). These features are also found in control runs in the CMIP5 models (*Østvand et al.*, 2014), and in CMIP5-simulations with discontinuous jumps of atmospheric CO_2 concentration, one observes relaxation to equilibrium where a fast response with time constant of 1 – 2 yr is followed by a slow decay that lasts for centuries (*Geoffroy et al.*, 2013). *Rypdal and Rypdal* (2014) demonstrated that all this can be modeled by replacing the exponential response function by a power law $G(t) = ct^{\beta/2-1}$ in Eq. (3). It can be shown that this corresponds to replacing the time derivative in Eq. (2) with a fractional derivative, hence we name it *the fractional EBM*.

Eq. (3) suggests that the standard, as well as the fractional, EBM can be viewed as a linear filter that transforms the forcing signal into temperature signal. In Fourier domain the equation takes the form $\tilde{T}(f) = \tilde{G}(f) [\tilde{F}(f) + \sigma \tilde{w}(t)]$, and for the PSD we get,

$$S(f) = |T(f)|^2 = |G(f)|^2 [|\tilde{F}(f)|^2 + \sigma^2]. \quad (4)$$

In the absence of deterministic forcing ($\tilde{F}(f) = 0$), we have $S(f) \sim |G(f)|^2$. If $G(t)$ is exponential then $S(f) = |G(f)|^2$ will be a Lorentzian, and the resulting stochastic process is the OU process. If $G(t)$ is the power law $G(t) \sim t^{\beta/2-1}$, then $S(f) = |G(f)|^2 \sim f^{-\beta}$, and the process is an fGn. In the absence of stochastic forcing, the filter represented by $|G(f)|^2$ will suppress only fluctuations on time scales smaller than τ if $G(t)$ is exponential, while the power-law filter will systematically suppress small scales and enhance large scales. Examples were shown by *Rypdal and Rypdal* (2014) where a time series for the total forcing throughout the last 130 yr is run through an exponential filter with $\tau = 4.3$ yr and a power-law filter with $\beta = 0.75$ (long-memory response). One observes that only the latter is able to reproduce a realistic response to the negative forcing due to volcanic eruptions (the negative spikes in the forcing signal). It also provides a better (although not perfect) fit to the large-scale trends in the observed temperature signal.

The long-memory response has important implications for prediction of future global temperature on century time scale. In Fig. 1 it is shown that in a medium pessimistic forcing scenario for the next

hundred years, the fractional, long-memory model predicts almost one degree higher temperature
 135 than the zero response-time model. The latter projection does not change much with an exponential
 response as long as τ is less than a decade.

The purpose of this paper is to assess the sensitivity of the attribution to the assumption of long,
 versus short, memory in the computation of the fingerprints associated to volcanic, solar, and an-
 thropogenic forcing. Sect. 2 describes briefly the multiple regression method and the regression
 140 diagnostics used, although these are very standard. Sect. 3.1 presents results based on instrumental
 surface temperature data and forcing reconstruction for the period 1880 – 2010 CE, and sect. 3.2
 presents the same analysis using a millennium-long multi-proxy reconstruction of Northern hemi-
 sphere temperature and ditto radiative forcing. Sect. 4 concludes and discusses the implications.

2 Data and methods

145 The forcing data in this paper are given as annual and global mean of the radiative forcing measured
 in Wm^{-2} . The data from the instrumental period 1880 – 2010 CE (Common Era) are those used
 by *Hansen et al.* (2005, 2011) and those for the reconstruction period 1000 – 1979 CE by *Crowley*
 (2000). The instrumental temperature data are given as annual and global mean surface temperature
 anomalies relative to AD 1880 (the HadCrut3 data set (*Brohan et al.*, 2006)), and the reconstructed
 150 temperature data as Northern Hemisphere annual means relative to 1000 CE (*Moberg et al.*, 2005).
 The forcing data are split up in solar, volcanic, and anthropogenic components. There are more
 recent instrumental data sets, but for the analysis in the present paper they will only provide unim-
 portant corrections. The reason for employing these older data sets is that it allows use of parameters
 estimated, and comparison to results obtained, in a recent paper (*Rypdal and Rypdal*, 2014).

155 In this paper we shall compare the effects of two different response filters; the zero response-time
 filter \mathcal{F}_{ZRT} and the long-range memory filter \mathcal{F}_{LRM} . Mathematically they represent two extremes,
 although we shall see that the LRM filter is a quite accurate representation of the actual response. If
 the total forcing is written as $F(t) = F_{\text{sun}}(t) + F_{\text{volc}}(t) + F_{\text{anthr}}(t)$, and \mathcal{F} is the filter operator, then
 we construct the *response function* (predictand);

$$160 \quad Q(t) = c_0 + c_1 \mathcal{F}F(t); \quad (5)$$

and determine the regression coefficients c_0, c_1 by a simple least-square fit. The response function
 $Q(t)$ is the fitted, filtered response to the total forcing $F(t)$ and can be considered as the best model
 we can make for the temperature signal with the filter \mathcal{F} , without allowing for different weights of
 the individual fingerprints. These fingerprints are defined as follows;

$$165 \quad \begin{pmatrix} S(t) \\ V(t) \\ H(t) \end{pmatrix} = c_1 \mathcal{F} \begin{pmatrix} F_{\text{sun}}(t) \\ F_{\text{volc}}(t) \\ F_{\text{anthr}}(t) \end{pmatrix}. \quad (6)$$

The responses $Q(t)$ are plotted for the two filter models in Fig. 2(a,c) and Fig. 6(a,c) to provide an indication of what the filtered response will be like if we do not allow for individual feedbacks to the different forcing components. The next step is to allow for such individual weights and determine them by construction of the linear predictand shown in Eq. (1). Our first choice is to leave out the AMO and ENSO predictors, leaving us with solar, volcanic, and anthropogenic forcing as predictors. With zero response time filter and these three predictors we have the ZRT 3P regression model. The corresponding case with LRM filter is the LRM 3P model. Including AMO and ENSO (five predictors) gives us the ZRT 5P and LRM 5P models. The weighted responses is our best estimate of climate *footprints* imposed by the forcing or internal modes characterised by the corresponding fingerprints.

The estimation of the regression coefficients and some diagnostics are done by the command *LinearModelFit* in *Mathematica*. For each predictand $Q(t)$ we provide the R^2 diagnostic (*coefficient of determination*), which measures the fraction of the total variance in the observed record that is explained by the predictand. As we move from one to three, and then to five, predictors (and ditto number of fitting parameters) we increase model complexity and will increase the explained variance. In model selection assessments we have model selection criteria based on information theory where the likelihood function is used as a measure of the goodness of the fit, which is subject to a penalty for model complexity. The most commonly used of these are the Akaike Information Criterion (AIC) and the Bayesian Information Criterion (BIC) (for an introduction to the concepts see *Burnham and Anderson* (2004)). Each of these criteria produces a real number that can be positive or negative, and the model giving the smaller number is in this particular sense preferable.

3 Results

3.1 Attribution from instrumental data

In this section we use the same instrumental global temperature data and the forcing data as employed by *Hansen et al.* (2011). The analysis is based on the annual mean time series.

3.1.1 Zero response time model

Fig. 2a (red curve) shows the predicted signal obtained by fitting the unfiltered forcing (more precisely; by fitting $Q(t)$ given by Eq. (5) subjected to the zero-response time filter \mathcal{F}_{ZRT}) to the instrumental GMST (blue curve). The fit is quite poor ($R^2 \approx 0.53$), and the response to the volcanic eruptions are obviously much stronger than observed. If we include an exponentially decaying response $\exp(-t/\tau)$, we will need a time constant τ larger than a decade in order to obtain realistic short-time responses to these eruptions (see *Rypdal* (2012)), provided we do not reduce the weight of the volcanic forcing. Another way of obtaining a better fit is to employ a multiple regression by using Eqs. (1) and (6). The result is shown in Fig. 2b. The fit is much better ($R^2 \approx 0.80$), but there is

200 a rather strong decadal oscillation attributable to the solar cycle. The redistribution of weights is apparent from Figs. 3a,b. The three fingerprints given in Fig. 3a are just a rescaling of the three forcing components by the same factor c_1 given by Eq. (6) with $\mathcal{F} = \mathcal{F}_{\text{ZRT}}$, and the red curve in Fig. 2a is just the unweighted superposition of these fingerprints plus the additive constant a_0 . The multiple three-component regression ZRT 3P is the superposition of the weighted fingerprints (i.e., the footprints) 205 shown in Fig. 3b. The regression amplifies the solar fingerprint $S(t)$ by a factor $f_{\text{sun}} \approx 2.10$, the anthropogenic fingerprint by $f_{\text{anthr}} \approx 1.58$, while the volcanic fingerprint is strongly attenuated with $f_{\text{volc}} \approx 0.22$. This strong attenuation is provoked by the unrealistically large short-time responses enforced by the zero response time model, and the suppression of the volcanic cooling is what has to be compensated by amplified solar and anthropogenic warming. Thus, for the ZRT response model 210 the strongly altered weights are most probably caused by an incorrect (too spiky) representation of the volcanic fingerprint.

3.1.2 The long-range memory response model

The ZRT response model is given by the delta function $G(t) = c\delta(t)$ and is obviously unrealistic. Next, we explore the effect of an LRM response function of the form $G(t) = (t/\mu)^{\beta/2-1}$. In 215 *Rypdal and Rypdal* (2014) a maximum-likelihood approach was applied to estimate $\mu = 0.84 \times 10^{-2}$ yr and $\beta = 0.75$ from the same instrumental temperature data and forcing data as used in the present paper. Fig. 2c shows the response variable given by Eq. (5) with $\mathcal{F}T(t)$ representing the LRM filter;

$$\mathcal{F}_{\text{LRM}} T(t) = \int_0^t [(t-t')/\mu]^{\beta/2-1} F(t') dt', \quad (7)$$

220 and $c_0 = 0.15 \times 10^{-2}$ K and $c_1 = 0.92$ determined by fitting Eq. (5) to the instrumental observation data. The fact that c_0 is close to zero and c_1 is close to unity shows that that least-square fit for these data give results compatible with the more general maximum-likelihood approach employed in *Rypdal and Rypdal* (2014). Compared to the ZRT-filtered response the explained variance R^2 is increased from 0.53 to 0.81. This is partly due to a better representation of the large-scale variability and a smaller immediate response to the volcanic eruptions due to the memory effects. The explained variance is only slightly increased by introducing variable weights on the solar, volcanic, and anthropogenic fingerprints ($R^2 \approx 0.83$), and the improvement is mostly caused by a suppression of the volcanic response. Compared to the fingerprints shown in Fig. 3c the volcanic footprint shown in Fig. 3d is reduced by a factor $f_{\text{volc}} \approx 0.53$, while solar footprint is only slightly amplified 230 by $f_{\text{sun}} \approx 1.18$ and the human footprint slightly attenuated by $f_{\text{anthr}} \approx 0.90$. The AIC and BIC are somewhat reduced, so this model is preferred compared to the unweighted LRM model, but the difference is not very large. With respect to explained variance and the information-theoretic selection criteria the ZRT 3P, LRM, and LRM 3P models are quite similar. However, visual inspection of the shape of the responses and footprints suggests that the ZRT 3P model results in suppression of

235 volcanic footprint and ditto amplification of the solar footprint that are unrealistically large. Similarly, the reduction of the volcanic footprint in the LRM 3P model by a factor of approximately 0.5 seems to give a much better fit to the short-time temperature around the large volcanic eruptions and suggests that the volcanic forcing signal in the forcing data may have been exaggerated.

3.1.3 Inclusion of internal modes

240 So far we have used only external forcing as predictors in our regression model. This means that all internal variability is interpreted as residual noise. However, some variability manifest in the global temperature is not adequately described as long-memory or short-memory noise. The ENSO signal is easily detected in the global temperature records, and even though El Niño or La niña events are unpredictable, the PSD of ENSO indices peak in the frequency range corresponding to periods between 2 and 7 yr. It is therefore common to include ENSO in attribution analyses (*Lean and Rind*, 2008, 2009; *Foster and Rahmstorf*, 2011). Another feature that appears impossible to explain with only forcing predictors is the low temperatures first decades of the nineteenth century and the high temperatures in the decades after World War-II. These anomalies may be compatible with an oscillation with period 60 – 70 yr, as discussed extensively by *Canty et al.* (2013). The statistical significance of this oscillation with respect to a long-memory null hypothesis for the noise background was discussed by *Østvand et al.* (2014), but has also been studied extensively by a number of authors with short-memory null models (*Ghil and Vautard*, 1991; *Schlesinger and Ramankutty*, 1994; *Plaut et al.*, 1995; *Polonski*, 2008). The mode has the same period and phase as the most prominent period in the AMO index, and thus it seems reasonable to introduce the AMO index as a predictor variable in addition to the Niño3 index if one wants to increase the explained variance. One could object that inclusion of temperature observations as predictor variables is a self-fulfilling trick. But as mentioned in the introduction, regression is not really about attributing observed variance to external causes but rather to attribute global temperature variability to a set of signatures (fingerprints). These may signify responses to forcing (causation), but also the footprint in the global temperature of observed climate signals like the North-Atlantic sea surface temperature or pressure differences across the tropical pacific.

But one should also bear in mind that climate forcing is a problematic concept, since the separation of forced from internal dynamics depends on what one defines as the “system” that is subject to external forcing. The reasoning above was based on thinking about ENSO and AMO as internal modes, and not as forcing. But one can also define the Earth surface/ocean mixed layer as the system, and this system can be forced by modes involving energy exchange between the surface/mixed layer and atmospheric systems (ENSO) and between the surface/mixed layer and the deep ocean. AMO is an example of the latter, and can be considered as the fingerprint of the forcing exerted on the ocean mixed layer from the Atlantic Meridional Overturning Circulation (AMOC) (*DelSole et al.*, 2013; *Medhaug and Furevik*, 2004; *Canty et al.*, 2013).

Using the LRM fingerprints for $S(t)$, $V(t)$, $H(t)$, and the AMO index for $A(t)$ in Eq. (1) (omitting the ENSO fingerprint), we find the response function shown in Fig 5a. It shows an improved fit with $R^2 \approx 0.86$, and the AIC and BIC are lower, suggesting that this LRM 4PA model is preferred to the LRM P3 model which does not include AMO as a predictor. The four fingerprints are shown in Fig. 5b, and do not show very large changes in the fingerprints relative to the LRM3 model shown in Fig. 3d, apart from a notable reduction in the volcanic footprint. **A similar effect of using AMO as a predictor was found by Canty et al. (2013).** Hence, the effect of including AMO as a predictor is mainly to raise the explained variance, but we also note a hiatus in the first decade of the 21st century. In Fig. 5c,d we show the effect of adding the Niño3 index as a predictor, in addition to AMO. The explained variance is raised to $R^2 \approx 0.89$, and the AIC/BIC are further reduced, suggesting that both AMO and ENSO are relevant explanatory variables and that including both contributes to a better statistical model. The hiatus post 2000 AD is even more pronounced when ENSO is included, due to the strong 1998 El Niño.

The total natural footprint (the sum of solar, volcanic, AMO and ENSO fingerprints) is dominated by the multidecadal oscillation with a weak growing trend caused by the growing trend in solar activity in the period 1880–1960. From Fig. 5d we observe that this trend in the solar footprint is very close to the trend in the anthropogenic footprint up to $t \approx 90$ (1970 AD), but after this time the solar footprint has no significant trend, while the trend in the anthropogenic footprint is approximately 0.13 K per decade. The anthropogenic footprint turns out to be very robust and quite insensitive to inclusion of natural modes in the regression analysis.

3.2 Attribution from multiproxy data

A similar analysis is made using the Northern Hemisphere multiproxy temperature reconstruction of Moberg et al. (2005) and the forcing reconstruction of Crowley (2000) for the period 1000–1979 AD. The data are given with annual resolution, but since the temperature data are effectively smoothed on time scales shorter than 5 yr, it seems unreasonable to use a zero response time model. Instead a short-memory response (SMR) model with exponential response function $G(t) = c \exp(-t/\tau)$ is employed. The parameters $c = 0.37$ K/yr and $\tau = 4.3$ yr were estimated by Rypdal and Rypdal (2014) using the instrumental data over the period 1880–2010 AD. As for the instrumental data we will also use the LRM model with parameters estimated from the instrumental data. By employing the models with these parameters we can examine how well the SMR model works versus the LRM model for a longer data set. This is interesting to do, because the SMR model employed to the instrumental data explains almost as large fraction of the variance as the LRM model (shown in Supplementary Material), and hence from those data the LRM is not strongly preferred to the SMR model based on the R^2 and AIC/BIC criteria only.

The SRM response is shown in Fig. 6a, and the corresponding fingerprints in Fig. 7a. The response function does not show a good fit ($R^2 \approx 0.17$) and AIC/BIC are large. Introduction of weighted

fingerprints increases the explained variance ($R^2 \approx 0.26$) and lowers AIC/BIC as shown in Fig. 6b. As shown in Fig. 3a,b this improvement comes about by a considerable reduction of the volcanic footprint ($f_{\text{volc}} \approx 0.45$) and from a very strong amplification of the solar footprint ($f_{\text{sun}} \approx 2.32$). The volcanic footprint is reduced to lower the variance due to the sharp spikes in the SRM-response to the volcanic forcing, and the solar footprint is amplified to reduce the unexplained variance from the cooling between the medieval warm anomaly (MWA) and the little ice age (LIA). The anthropogenic footprint is also amplified ($f_{\text{anthr}} \approx 1.48$). However, the LRM model increases the explained variance to $R^2 \approx 0.39$, and drastically reduces AIC/BIC, even without introducing weighted fingerprints. This is shown in Fig. 6c, and demonstrates that the LRM model is strongly preferred over the SRM model when we consider time scales up to a millennium. The consistency of the LRM model is supported by the observation that introduction of weighted fingerprints introduces weights moderately different from unity. The main change is an enhancement of the solar footprint ($f_{\text{sun}} \approx 1.44$) at the expense of the volcanic ($f_{\text{volc}} \approx 0.78$). The anthropogenic footprint is virtually unchanged ($f_{\text{anthr}} \approx 0.99$). This tendency to enhanced solar, reduced volcanic, and only slightly affected anthropogenic footprints is consistent with what was observed for from the LRM model applied to the instrumental data.

Fig. 7d suggests that the temperature difference between the maximum of the MWA (1000 CE) and the minimum of the LIA (1700 CE) can be mainly attributed to volcanic cooling, while the warming from the LIA until 1970 CE is attributed to solar and anthropogenic influence. The latter is also consistent with what we observe from Fig. 7c.

For all response models the explained variance is considerably lower for the reconstruction data than for the instrumental data. This is mainly due to the strong anthropogenic trend in the instrumental period. This trend dominates the variance and is very well predicted, hence it increases the predicted variance.

3.3 Effect of initial state and prehistory

By defining the fingerprints as integrals over the time interval $(0, t)$ we implicitly assume that there is no influence of past forcing from the interval $(-\infty, 0)$, i.e., we effectively assume zero forcing in prehistory. For the exponential (SRM) response function this has no consequence, because this response function corresponds to the simple EBM which is just a first-order ordinary differential equation whose solution only depends on the initial temperature (see discussion in *Rypdal and Rypdal (2014)*). For the power-law response, prehistory matters in principle, since the corresponding differential equation contains a fractional derivative. But even for the simple SMR response we cannot faithfully assume that the initial forcing is zero, since this corresponds to assuming that the climate system is in equilibrium at time $t = 0$. This may have some surprising implications, so some detail can be appropriate. Consider as an illustration the simple zero-dimensional EBM

$$C \frac{dT}{dt} = -\epsilon \sigma_S T^4 + I(t), \quad (8)$$

where T is surface temperature in Kelvin, C is an effective heat capacity per area of the Earth's surface, σ_S is the Stefan-Boltzmann constant, ϵ is an effective emissivity of the atmosphere, and $I(t)$ is the incoming radiative flux density at the top of the atmosphere. Let $T_0 = T(t=0)$, $I_0 = I(t=0)$,
 345 $T = T_0 + \tilde{T}$, and $I = I_0 + F$. **Note that F here is the perturbation of the radiative flux with respect to the initial flux I_0 and not with respect to the flux that would be in equilibrium with the initial temperature T_0 .** The linearised equation for the temperature change relative to the temperature T_0 is

$$C \frac{d\tilde{T}}{dt} = -(4\epsilon\sigma_S T_0^3)\tilde{T} + (I_0 - \epsilon\sigma_S T_0^4) + F(t). \quad (9)$$

The quantity $I_0^{(eq)} \equiv \epsilon\sigma_S T_0^4$ represents the incoming flux required to balance the outgoing long-wave radiation (OLR) from the top of the atmosphere when the surface temperature is T_0 . This is
 350 not necessarily equal to the actual incoming flux at time $t=0$, so the difference $F_0 = I_0 - \epsilon\sigma_S T_0^4$ represents the initial forcing (or the initial imbalance of radiative flux density). By definition $F(0) = I(0) - I_0 = 0$, and represents the sum of various forcing components that we have used to establish the forcing fingerprints, as they are all defined to be zero at $t=0$. The solution to Eq. (9) takes the
 355 form

$$\tilde{T} = F_0 \int_0^t G(t-t') dt' + \int_0^t G(t-t') F(t') dt'. \quad (10)$$

To understand the implications let us look at the case where $F(t)$ is a stationary stochastic process, implying that the expectation value $E[F(t)]$ is independent of t . Eq. (10) then describes realisations of the response to this forcing under the condition that the initial radiative imbalance is F_0 . The
 360 expectation (ensemble average) of this response is then

$$E[\tilde{T}] = (F_0 + E[F]) \int_0^t G(t-t') dt'. \quad (11)$$

If we assume that the response is also stationary this equation implies that $E[F] = -F_0$. What this means is that if the initial imbalance is a fluctuation around a stationary climate state, but everything is measured as perturbations relative to the *initial* state, then the mean of the forcing F in the future
 365 will balance the initial forcing F_0 to render \tilde{T} finite. On the other hand, if F and T are not stationary processes, this is no longer true. Consider for instance that the imbalance F_0 is the result of a step in radiative influx just prior to $t=0$. If the radiative flux is held constant after this step we would have that $F(t) = 0$ for $t > 0$, and the evolution would be given by the first integral in Eq. (10).

For an exponential response function this contribution converges to a constant for $t \gg \tau$, but for
 370 a power-law response it takes the form $\tilde{T} \sim t^{\beta/2}$. The divergence as $t \rightarrow \infty$ is of course unphysical. It reminds us that that the power-law response is an idealised representation of the response of a system with a large range of response times, and that it must be cut-off at some time scale (Rypdal and Rypdal, 2014). But it illustrates that if parts of the climate system responds very slowly there

may be a strong influence of an initial energy imbalance throughout the entire temperature record
375 under consideration.

The effect of past forcing is a less serious problem. It was shown in *Rypdal and Rypdal* (2014) to be negligible over the instrumental period, using information about forcing and temperature over the past millennium. We have not done a similar computation for the millennium period, since reliable global scale reconstructions for the previous millennia are not available. However, for past forcing
380 to have a long-term effect, the climate system must have been driven strongly away from radiative equilibrium over an extended period. This is the case in the anthropocene, but is not believed to have occurred throughout earlier millennia in the holocene.

We do not have direct physical information about the radiative flux imbalance in year 1000 CE, but the high temperatures during the MWA could suggest that OLR was higher than the incoming flux at
385 the start of the subsequent cooling. What we can do by means of attribution techniques is to include $T_{F_0} = F_0 \int_0^t G(t-t') dt'$ as an extra fingerprint and estimate F_0 along with the other regression coefficients. The results are shown in Fig. 8. The total response in Fig. 8a explains more variance than the model that does not include T_{F_0} , and the AIC/BIC prefers this model. In particular, the large discrepancy between explained and observed variability during the first century of the record
390 (during the MWA, 1000-1100 CE) in the other models has disappeared in this long-memory four-predictor (LRM 4P) model. Fig. 8b shows a strong reduction in the volcanic footprint, because the long-term trend imposed by F_0 provides the cooling previously attributed to volcanic activity. It is quite apparent from Fig. 8a that the estimated response exhibits weak short-term response to volcanic eruptions, but the estimated $f_{\text{volc}} \approx 0.28$ is only 30% lower than what was estimated from
395 the LRM 5P model applied to the instrumental data (Fig. 5d). The volcanic footprint may have been somewhat underestimated in Fig. 8a, simply because the short-term response does not contribute very much to the total variance. However, recent work on detection and attribution which compare multiproxy reconstructions with paleoclimatic simulations with general circulation models show that the models seem more sensitive on short time scales to volcanic eruptions than observed in
400 the reconstructions (*Schurer et al.*, 2013). Many explanations can be offered for this observation, and one could be that volcanic forcing used in the models, or its efficacy, has been systematically overestimated. Hence, it is difficult to rule out that the tendency shown in Fig. 8 could be more than an analysis artifact.

4 Conclusions

405 Standard linear, multiple regression has been applied to instrumental and multiproxy reconstructed global and northern hemispheric temperatures, using fingerprints derived from reconstructed forcing and internal mode indices as predictor variables. The fingerprints have been derived from simple short-memory and long-memory response models. The regression coefficient for the volcanic fin-

gerprint will be strongly suppressed by zero-response time and short memory response models, but
 410 the explained variance is still around 80%. The modeling of *Lean and Rind* (2008) is similar to our
 ZRT 3P, but with inclusion of finite time delays and ENSO as an additional predictor. Their results
 shown in their Fig. 2 are quite similar to the ZRT 3P results shown in Fig. 2b and Fig. 3b, with an
 explained variance of 76%. Hence, the inclusion of ENSO and finite time delay without the memory
 smoothing of the response does not seem to improve the explained variance, while the increased
 415 model complexity necessarily will increase the AIC/BIC scores and make the model less preferable.
 The model of *Lean and Rind* (2008) suffers from the same feature as the the ZRT 3P model that
 it overestimates the 11-yr solar cycle response by not taking into account the attenuating effect of
 long-memory response to oscillatory forcing on decadal time scale. In *Rypdal* (2012) it was shown
 that the large solar cycle response of 0.2 K peak-to-peak detected by *Camp and Tung* (2007) in
 420 global surface temperatures in the period 1959 – 2004 CE are largely attributed to three volcanic
 eruptions incidentally taking place in the descending phase of solar cycles. By correcting for the
 responses to these eruptions there will be a considerably weaker response to the solar cycle in the
 global temperature series.

Multiple regression based on fingerprints derived from long-memory response models, and in
 425 particular with AMO and ENSO included as predictors, yields a response variable that explains 89%
 of the total variance of the instrumental data set for 1880–2010 AD. Relative to the forcing data
 set employed for this period the solar footprint is modified by a factor $f_{\text{sun}} \approx 1.23$, the volcanic
 footprint by a factor $f_{\text{volc}} \approx 0.41$, and the anthropogenic footprint by a factor $f_{\text{anthr}} \approx 0.77$. In the
 instrumental period the natural variability is dominated by an internal oscillation with period 60–
 430 70 yr, and this oscillation dominates over the forced trend up to 1970 CE. The forced trend before
 1970 is shared in equal proportion between solar and anthropogenic footprints. After 1970 AD the
 trend in the anthropogenic footprint is approximately 0.13 K per decade, but the trend in the total
 response has been amplified by the upward phase of the AMO footprint and the strong El Niño in
 1998. The combination of these footprints and that of the Mount Pinatubo eruption in 1991 AD
 435 yields a total response function showing a hiatus in the years 2002–2010 CE. *Lean and Rind* (2008,
 2009) attribute much of this hiatus to the descending solar cycle, while in the present analysis shown
 in Fig. 5 the maximal phase of the AMO in 2010 CE and the 1998 El Niño give more important
 contributions. A recent update of the sea-surface temperature (SST) has cast doubt about the reality
 of the hiatus in global temperature (*Karl et al.*, 2015). This is consistent with the present results,
 440 since these corrections to the SST also pertain to the AMO and ENSO fingerprints. Correction of
 these fingerprints will probably eliminate the hiatus in the LRM 5P response shown in Fig. 5c. The
 solar-cycle fingerprint, however, is unaffected by these corrections, so in the model of *Lean and*
Rind (2008, 2009) the hiatus will persist in their modeled response despite these corrections of the
 observed temperature.

445 By including the AMO as additional predictor in the LRM-model response (but leaving out ENSO) the volcanic response is reduced by a factor two. This somewhat surprising result is due to the structure of the volcanic forcing over the instrumental period, with a five decade long period of low volcanic forcing prior to the Mount Agung eruption in 1963, and a series of major disruptions including El Chichón (1982) and Pinatubo (1991). Without the AMO the post World-War II cooling
450 will be attributed exclusively to volcanic cooling, while inclusion of AMO will attribute about half of this cooling to the low phase of the AMO. This finding is in close agreement with those of *Canty et al.* (2013), and in our paper it depends on the LRM character of the response, which we believe is strongly related to the overturning circulation. Without this delayed response (as illustrated by the results for the ZRT 3P model in Fig. 3) the volcanic response would be anomalously low both with
455 and without AMO.

For the millennium reconstruction the short-memory response with time constant 4.3 yr is unable to reproduce the reconstructed long time-scale variability. The long-memory response offers two viable models for the large-scale variability. One where most of the cooling from the MWA to the LIA is attributed to volcanic activity. The other attributes more of this cooling to a negative radiative
460 imbalance at the end of the MWA, represented as a negative initial forcing at 1000 AD, and giving rise to a downward temperature trend throughout the last millennium. Both explanations require that there is a significant long-memory impact up to millennium time scales.

The regression examples shown in this paper demonstrate that the results of attribution studies based on multiple, linear regression depend strongly on the memory properties of the models employed to define the fingerprints. Models including long-term memory in the response tend to explain more of the observed variance and have better scores on information-theoretic model selection tests. Results also vary with the number and nature of the fingerprints used as predictors. Nevertheless, there are some tendencies that seem to be robust throughout. The weight of the anthropogenic footprint is not systematically changed by treating the individual forcing components as independent
470 predictors, and almost all of the global warming since 1970 CE can be attributed to it. The solar footprint is enhanced by a factor of approximately two with short-memory response, but is not changed a lot with long-memory response. The volcanic footprint is strongly suppressed with short-memory response, and is also somewhat weaker with long-memory response. Even though the solar footprint is enhanced in all models, none of them attributes the Little Ice Age primarily to solar variability.

475 *Acknowledgements.* This work was funded by project no. 229754 under the the Norwegian Research Council KLIMAFORSK programme. The author thanks Tine Nilsen and Hege-Beate Fredriksen for useful comments.

References

- Blender, R. and Fraedrich, K.: Long time memory in global warming simulations, *Geophys. Res. Lett.*, 30, 1769, doi: 10.1029/2003GL017666, 2003.
- 480 Brohan, P., Kennedy, J. J., Harris, I., Tett, S. F. B., and Jones, P. D.: Uncertainty estimates in regional and global observed temperature changes: A new data set from 1850, *J. Geophys. Res.*, 111, D12 106, 2006.
- Burnham, K. P., and Anderson, D. R.: Multimodel inference: understanding AIC and BIC in model selection, *Sociological Methods & Research* 33, 261–304, doi:10.1177/0049124104268644, 2004.
- Camp, C. D., and Tung, K. K.: Surface warming by the solar cycle as revealed by the composite difference
485 projection, *Geophys. Res. Lett.*, 34, L14703, doi:10.1029/2007GL030207, 2007.
- Canty, T., Mascioli, N. R., Smarte, M. D., and Salawitch, R. J.: An empirical model of global climate – Part 1: A critical evaluation of volcanic cooling, *Atmos. Chem. Phys.*, 13, 3997–4031, doi:10.5194/acp-13-3997-2013, 2013.
- DelSole, T., Tippet, M. K., and Shukla, J.: A significant Component of Unforced Multidecadal Variability in
490 the Recent Acceleration of Global Warming, *J. Climate*, 24, 909–926, doi: 10.1175/2010JCLI3659.1, 2011.
- Crowley, T. J., 2000: Causes of Climate Change Over the Past 1000 Years. *Science*, 289 (5477), 270–277, 2000.
- Foster, G. and Rahmstorf, S.: Global temperature evolution 1979–2010, *Environ. Res. Lett.*, 6, 044022, doi:10.1088/1748-9326/6/4/044022, 2011.
- Geoffroy, O., Saint-Martin, D., Olivé, D. J. L., Voldoire, A., Bellon, G., and Tytca, S.: Transient Climate
495 Response in a Two-Layer Energy-Balance Model. Part I: Analytical Solution and Parameter Calibration Using CMIP5 AOGCM Experiments, *J. Climate*, 6, 1841–1857, doi:10.1175/JCLI-D-12-00195.1, 2013.
- Ghil, M., and Vautard, R.: Interdecadal oscillations and the warming trend in global temperature time series, *Nature*, 350, 324–327, doi:10.1038/350324a0, 1991.
- Hansen, J., Nazarenko, L., Ruedy, R., Sato, M., Willis, J., Del Genio, A., Koch, D., Lacis, A., Lo, K., Menon, S.,
500 Novakov, T., Perlwitz, J., Russel, G., Schmidt, G. A., Tausnev, N.: Earth's energy imbalance: Confirmations and Implications, *Science*, 308, 1431–1435, doi:10.1126/science.1110252, 2005.
- Hansen, J., Sato, M., Kharecha, P., von Schuckmann, K.: Earth's energy imbalance and implications, *Atmos. Chem. Phys.*, 11, doi:10.5194/acp-11-13421-2011, 2011.
- Hegerl, G. C., von Storch, H., Hasselmann, K., Santer, B. D., Cubasch, U., Jones, P. D.: Detecting greenhouse
505 gas induced climate change with an optimal fingerprint method, *J. Climate*, 9, 2281–2306, 1996.
- Lean, J. L. and Rind, D. H.: How natural and anthropogenic influences alter global and regional surface temperatures: 1889 to 2006, *Geophys. Res. Lett.*, 35, L18701, doi:10.1029/2008GL034864, 2008.
- Lean, J. L. and Rind, D. H.: How will Earth's surface temperature change in future decades? *Geophys. Res. Lett.*, 36, L15708, doi:10.1029/2009GL038932, 2009.
- 510 Medhaug, I., and Furevik, T.: North Atlantic 20th century multidecadal variability in coupled climate models: sea surface temperature and overturning circulation, *Ocean. Sci.*, 7, 389–404, doi: 10.5194/os-7-389-2011, 2011.
- Meehl, G. A., Washington, W. M., Amman, C. M., Arblaster, J. M., Wigley, T. M., and Tebaldi, C.: Combinations of Natural and Anthropogenic Forcings in Twentieth-Century Climate, *J. Climate*, 17, 3721–3727, 2004.

- 515 Moberg, A., Sonechkin, D. M., Holmgren, K., Datsenko, N. M., and Karlen, W.: Highly variable Northern Hemisphere temperatures reconstructed from low- and high-resolution proxy data, *Nature*, 433, 613–617, 2005.
- Plaut, G., Ghil, M., and Vautard, R.: Interannual and interdecadal variability in 335 years of central England temperatures, *Science*, 286, 710–713, doi:10.1126/science.268.5211.710, 1995.
- 520 Polonski, A. B.: Atlantic multidecadal oscillation and its manifestation in the Atlantic-European region, *Physical Oceanography*, 18, 227–236, doi:10.1007/s11110-008-9020-8, 2008.
- Rypdal, K. (2012) Global temperature response to radiative forcing: Solar cycle versus volcanic eruptions, *J. Geophys. Res.*, 117, D06115, doi:10.1029/2011JD017283, 2012.
- Rypdal, K., Østvand, L., and Rypdal, M.: Long-range memory in Earth’s surface temperature on time scales
525 from months to centuries, *J. Geophys. Res.*, 118, doi:10.1002/jgrd.50399, 2013.
- Rypdal, M., and Rypdal, K.: Long-memory effects in linear-response models of Earth’s temperature and implications for future global warming, *J. Climate*, 27, 5240–5258, doi:10.1175/JCLI-D-13-00296.1, 2014.
- Schlesinger, M. E. and Ramankutty, N.: An oscillation in the global climate system of period 65–70 years, *Nature*, 367, 723–726, 1994.
- 530 Schurer, A. P., Hegerl, G. C., Mann, M. E., Tett, S. F. B., Phipps, S. J.: Separating Forced from Chaotic Climate Variability over the Past Millennium, *J. Climate*, 26, 6954–6973, doi:10.1175/JCLI-D-12-00826.1, 2013.
- Thomas, R. K., et al.: Possible artifacts of data biases in the recent global surface warming hiatus, *Science*, June 4, 2015 doi:10.1126/science.aaa5632, doi:10.1175/JCLI-D-12-00826.1, 2013.
- Østvand, L., Nilsen, T., Rypdal, K., Divine, D., and Rypdal, M.: Long-range memory in internal and forced
535 dynamics of millennium-long climate model simulations, *Earth. Syst. Dynam.*, 5, 295–308, doi:10.5194/esd-5-295-2014, 2014.
- Østvand, Rypdal, K., and Rypdal, M.: Statistical significance of rising and oscillatory trends in global ocean and land temperature in the past 160 years, *Earth. Syst. Dynam.*, 5, 327–362, doi:10.5194/esdd-5-327-2014, 2014.

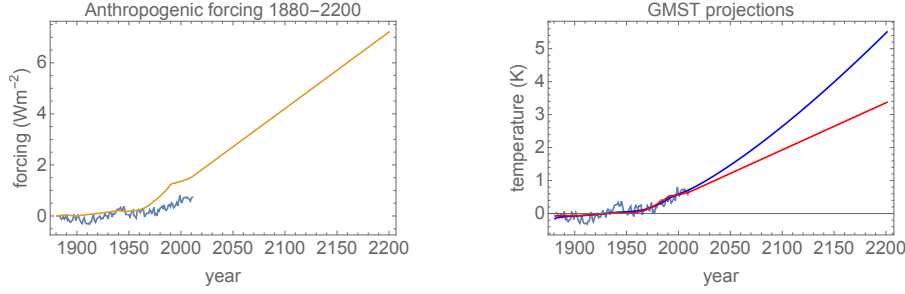


Figure 1. The light blue curves in both panels are observed global temperature in the period 1880 – 2010 CE. The orange curve on the left is the historic anthropogenic forcing extended with an exponential growth in atmospheric CO_2 -concentration ending around 700 ppm a hundred years from now. The red curve on the right shows the projected temperature from a standard EBM with $\tau = 0$, and the blue curve from a fractional EBM with $\beta = 0.75$. The difference between the two projections in year 2100 CE is almost one degree Celcius.

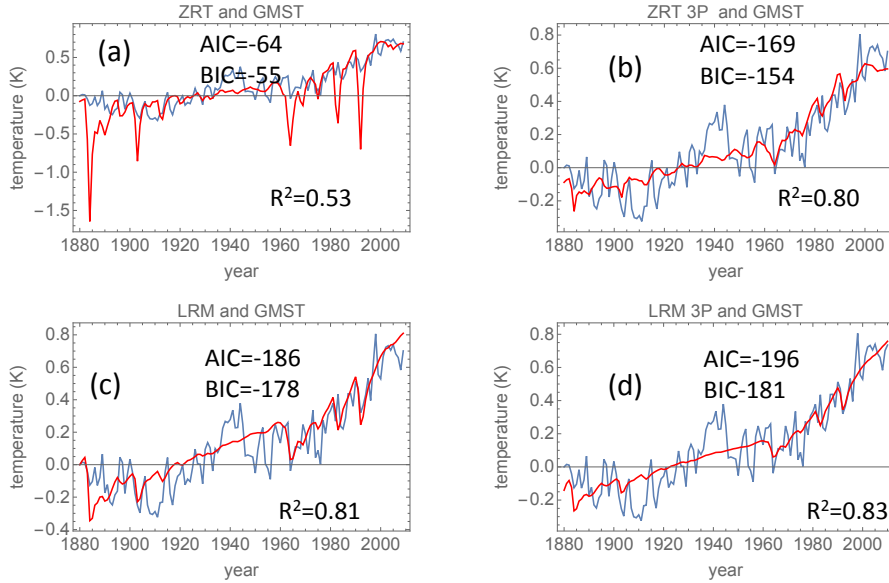


Figure 2. Blue curve in all panels is the instrumental GMST recorded in the period 1880 – 2010 CE. (a): The ZRT regressed signal $Q(t)$ defined in Eq. (5) with \mathcal{F} the ZRT (identity) filter and $F(t)$ the total forcing. (b): The ZRT 3P regressed signal according to Eq. (1) without AMO and ENSO as predictors. (c): The LRM regressed signal $Q(t)$ defined in Eq. (5) with \mathcal{F} the LRM filter. (d): The LRM 3P regressed signal according to Eq. (1) without AMO and ENSO as predictors.

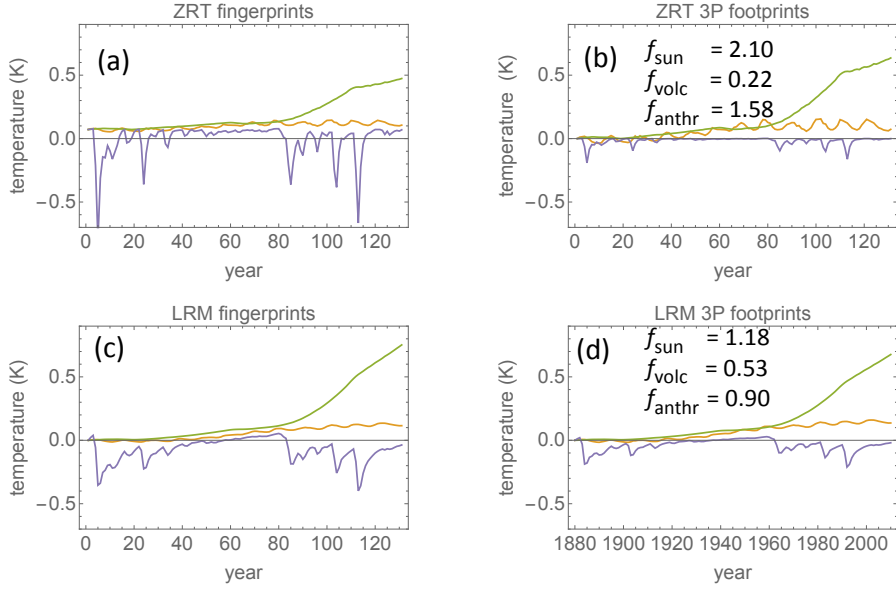


Figure 3. Fingerprints and footprints for the instrumental temperature 1880 – 2010 CE. (a): The application of Eq. (6) with \mathcal{F} the ZRT filter to the individual forcing components; $F_{\text{sun}}(t)$ (yellow), $F_{\text{volc}}(t)$ (magenta), $F_{\text{anthr}}(t)$ (green) to produce the fingerprints $S(t)$, $V(t)$, and $H(t)$ for the ZRT filter. (b): The footprints $f_{\text{sun}} S(t)$ (yellow), $f_{\text{volc}} V(t)$ (magenta), and $f_{\text{anthr}} H(t)$ (green) of ZRT 3P regressed signal. (c): The same as in (a) but with the LRM filter. (d): The same as in (b) but with the LRM filter.

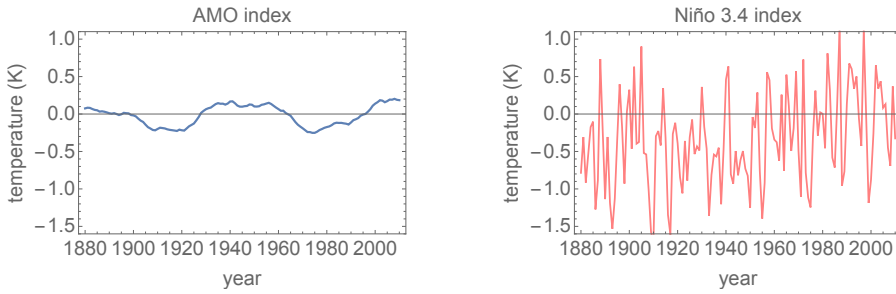


Figure 4. (a): The AMO index with annual resolution 1880 – 2010 CE. (b): The Niño 3.4 index for the same period as in (a).

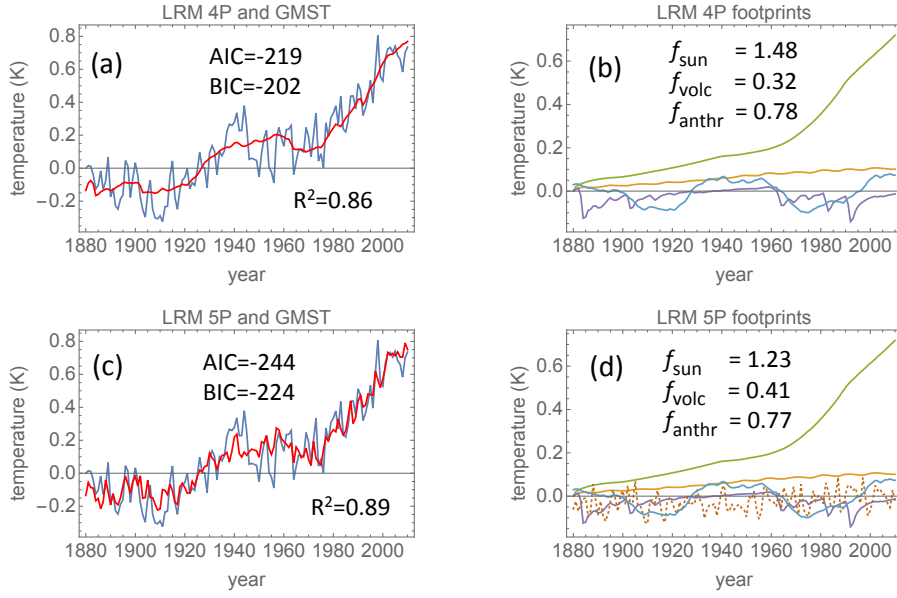


Figure 5. (a): The LRM 4PA signal, i.e., the regressed signal according to Eq. (1) including the three forcings and AMO (but not ENSO) as predictors. (b): The footprints $f_{\text{sun}} S(t)$ (yellow), $f_{\text{volc}} V(t)$ (magenta), $f_{\text{anthr}} H(t)$ (green), and $f_{\text{AMO}} A(t)$ of LRM 4PA regressed signal. (c): The LRM 5P signal, i.e., the same as in (a), but with the ENSO signal added in the regression. (d): The LRM 5P footprints, i.e., the same as in (b), but with the ENSO signal added in the regression. The ENSO footprint is the orange dotted curve.

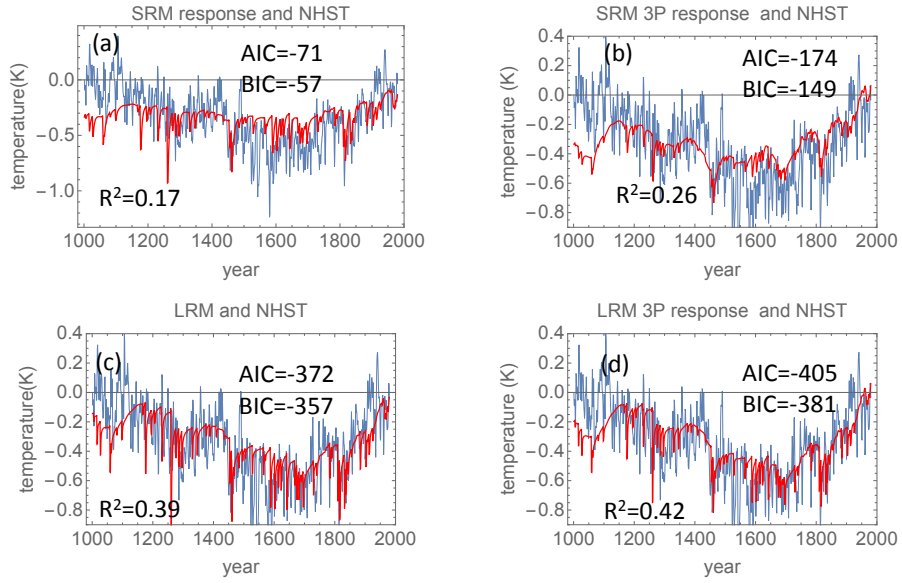


Figure 6. Blue curve in all panels is the Moberg reconstructed temperature for the Northern Hemisphere plotted for the interval 1000 – 1979 CE. (a): The SRM regressed signal $Q(t)$ defined in Eq. (5) with \mathcal{F} the SRM filter and $F(t)$ the total forcing. (b): The SRM 3P regressed signal according to Eq. (1) without AMO and ENSO as predictors. (c): The LRM regressed signal $Q(t)$ defined in Eq. (5) with \mathcal{F} the LRM filter. (d): The LRM 3P regressed signal according to Eq. (1) without AMO and ENSO as predictors.

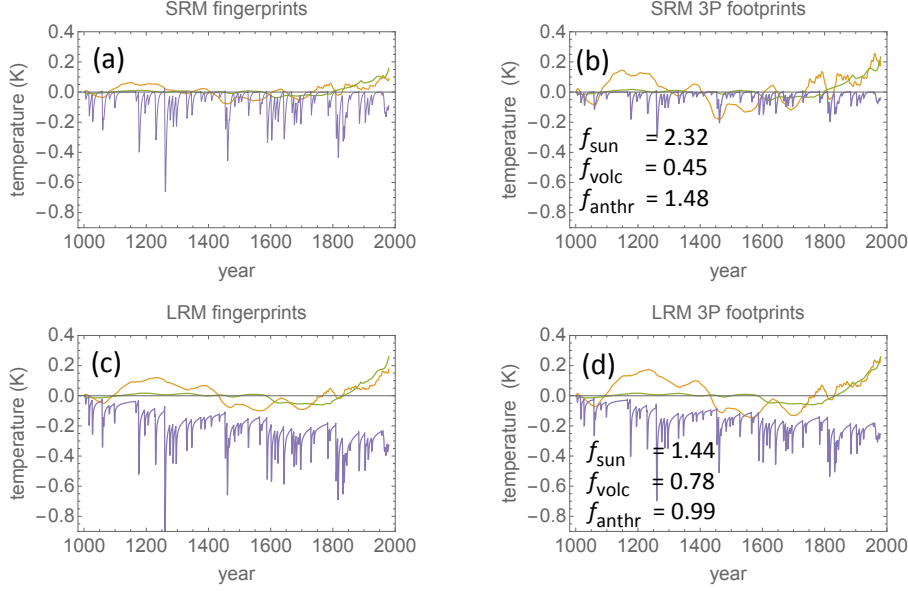


Figure 7. Fingerprints and footprints for the Northern Hemisphere temperature for 1000 – 1979 CE. The application of Eq. (6) with \mathcal{F} the SRM filter to the individual forcing components; $F_{\text{sun}}(t)$ (yellow), $F_{\text{volc}}(t)$ (magenta), $F_{\text{anthr}}(t)$ (green) to produce the fingerprints $S(t)$, $V(t)$, and $H(t)$ for the SRM filter. (b): The footprints $f_{\text{sun}} S(t)$ (yellow), $f_{\text{volc}} V(t)$ (magenta), and $f_{\text{anthr}} H(t)$ (green) of SRM 3P regressed signal. (c): The same as in (a) but with the LRM filter. (d): The same as in (b) but with the LRM filter.

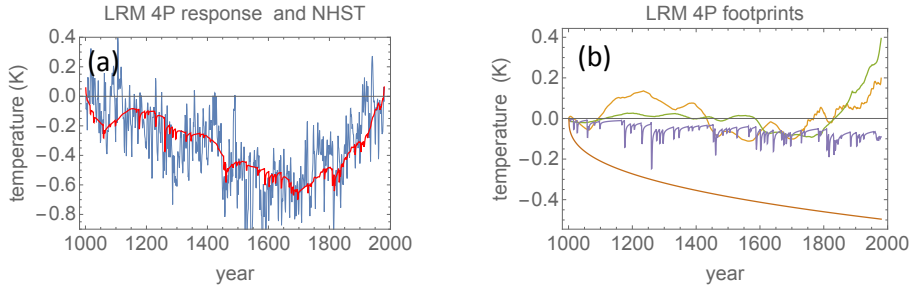


Figure 8. (a): The same as in Fig. 6d, but with inclusion of the LRM response T_{F_0} to the initial forcing F_0 as a predictor. (b): The corresponding footprints. The brown smooth curve is T_{F_0} .